Novel cost-effective approach to produce nano-sized contact openings in an aluminum oxide passivation layer up to 30 nm thick for CIGS solar cells.

Iryna Kandybka [1,2,3,4], **Gizem Birant** [2,3,4*], **Jessica de Wild** [2,3,4], **Dilara G. Buldu** [2,3,4], **Thierry Kohl** [2,3,4], **Ragha T. Eachambadi** [5], **Guy Brammertz** [2,3,4], **Jean V. Manca** [5], **Marc Meuris** [2,3,4], **Jef Poortmans** [2,3,4,6,7] and **Bart Vermang** [2,3,4]

[1] École Centrale de Lyon, 36 av. Guy de Collongue, 69134 Écully, France.
[2] Institute for Material Research (IMO), Hasselt University (partner in Solliance), Wetenschapspark 1, 3590 Diepenbeek, Belgium
[3] Imec division IMOMEC (partner in Solliance), Wetenschapspark 1, 3590 Diepenbeek, Belgium
[4] EnergyVille, Thorpark, Poort Genk 8310 & 8320, 3600, Belgium
[5] UHasselt - X-LAB, Agoralaan, 3590 Diepenbeek, Belgium
[6] imec (partner in Solliance), Kapeldreef 75, Leuven, 3001, Belgium
[7] Department of Electrical Engineering, KU Leuven, Kasteelpark Arenberg 10, 3001, Heverlee, Belgium.
*e-mail: gizem.birant@imec.be

Abstract

This work presents a novel method of local contact openings formation in an Aluminum Oxide (Al_2O_3) rear surface passivation layer by the selenization of the Lithium Fluoride (LiF) salt on top of the Al_2O_3 for ultra-thin CIGS solar cells. This study introduces the potentially cost-effective, fast, industrially viable, and environmentally friendly way to create the nano-sized contact openings with the homogeneous distribution in the thick, i.e., up to 30 nm, Al_2O_3 passivation layer. The passivation layer is deposited by atomic layer deposition (ALD), while the LiF layer is spin-coated. Selenization is done in the H_2Se atmosphere and the optimal process parameters are deduced to obtain nano-sized and uniformly allocated openings as confirmed by scanning electron microscopy (SEM) images. The contact openings were produced in the different thicknesses of the alumina layer from 6 nm to 30 nm. Furthermore, the aluminum oxide rear surface passivation layer with the contact openings was implemented into ultra-thin CIGS solar cell design, and one trial set was produced. We demonstrated that the created openings facilitate the effective current collection through the dielectric Al_2O_3 layer up to 30 nm thick. However, the upper limit of aluminum oxide thickness in which the contact openings can be created by the described method is not established yet. The produced passivated CIGS solar cells show increased EQE response due to the optical enhancement of the passivated cells. However, the production of solar cells on the Al_2O_3 passivation layer with the openings created by selenization of LiF is not optimized yet.

1. Introduction

Among existing thin-film solar cell (SC) technology, the most efficient is Copper Indium Gallium (di)Selenide - Cu(In, Ga)Se$_2$ (CIGS) with a world record of 23.35% in lab-scale [1]. However, the usage of rare materials with high price is the limiting factor for industrial production of CIGS SC as 1 GW CIGS photovoltaic module requires about 31 tons of indium [2]. One way to decrease the production cost is to use an ultra-thin absorber layer with a thickness of less than 1 μm. However, for ultra-thin CIGS SC achieving efficiencies as high as the thick one is highly challenging due to increased back-contact recombination and incomplete light absorption [3].

Rear surface passivation is a proven method to enhance the SC efficiency by decreasing the level of rear surface recombination and increasing the reflectance at the rear-contact. One way to passivate the rear surface is using a dielectric material in between CIGS absorber layer and back contact. Aluminum Oxide (Al$_2$O$_3$) is one of the most efficient materials used for this aim [4]–[7]. Such a dielectric layer acts as a barrier for charge carriers as well as for Sodium (Na) diffusion from the soda-lime glass (SLG) substrate. However, to be able to collect charge carriers from the absorber layer electrical contact is facilitated by local point contact openings.

Existing contacting approaches applied to Al$_2$O$_3$ rear surface passivation layer are previously described [8]. However, these methods either significantly increase production expenses, i.e., e-beam lithography, photolithography, nano-imprint lithography or using Mo nanoparticles, or are limited to a thin alumina layer of 5 nm [8].

It is published recently that alkali salt (Sodium Fluoride, NaF) on top of the passivation layer (alumina) during CIGS deposition process leads to the openings creation in the passivation layer due to the selenization [9], [10]. However, exceeding 6 nm alumina layer is not possible to obtain sufficient openings with NaF [10]. After trying different alkali salts to determine their effects on the creation of the openings, we investigated that LiF is one of the best options to create nano-sized openings in the thicker passivation layers. As a result, this work investigates the new cost-effective method of local point contact openings creation in the Al$_2$O$_3$ rear surface passivation layer by Lithium Fluoride (LiF) salt selenization for ultra-thin CIGS SC.

2. Method

2.1. Openings creation in the Al$_2$O$_3$ layer

The used substrates consist of SLG with a barrier layer (SiO$_x$N$_y$) and a sputtered Mo layer that serves as back contact for the final device. The layers' thicknesses in the SLG/SiO$_x$N$_y$/Mo stack are approximately 3 mm, 50 nm, and

Table 1. The annealing parameters used for selenization of the samples with the Al$_2$O$_3$ layer. The temperature and time are given for each alumina layer thickness.

Al$_2$O$_3$ layer thickness, nm	Temperature, °C	Time, s
6	540	450
8, 10, 15	550	500
20, 25, 30	550	560

300 nm, respectively. To remove possible organic residues and native oxide on top of the Mo layer, the substrate surface is cleaned with, first, isopropanol and, second, ammonia solution. The alumina layer is deposited on top of the Mo back contact by ALD at 300°C. The precursors used for a process are H$_2$O and trimethylaluminum (TMA). The thickness of the alumina layer is determined by the number of the cycles with a nm/cycle rate of 0.17 as determined for Si substrate. The tested Al$_2$O$_3$ thicknesses are 6 nm, 8 nm, 10 nm, 15 nm, 20 nm, 25 nm, and 30 nm. A water solution (1.6 M) of LiF is spin-coated on top of the Al$_2$O$_3$ layer by at 3000 rpm with an acceleration of 3000 rpm/s. An Annealsys modulus is used for samples selenization. During the selenization process, 4 samples are placed into the tool using a graphite sample holder. The samples are heated in H$_2$Se atmosphere and are annealed at the specific temperature/time given in **Table 1**. The parameters are experimentally investigated by aiming the lowest thermal budget possible that results in repeatable openings profile, see section 3.1 for details.

2.2. Rear surface passivated (RSP) CIGS SCs

2 types of the SC devices are produced: a reference and a rear surface passivated (RSP) device, see **Figure 1**. For the RSP device the Al$_2$O$_3$ passivation layer with openings is implemented as described in the previous part, while for the reference sample the CIGS layer is deposited on the Mo back contact. An ultra-thin 500 nm CIGS layer is co-evaporated from open-boat sources in a high-vacuum chamber. The thin 5 nm NaF layer is deposited further as alkali post deposition treatment (PDT) which is known to enhance the cell performance [11]. Cadmium Sulfide (CdS) buffer layer is deposited by Chemical bath deposition (CBD) and is followed by intrinsic Zinc Oxide (ZnO) and Aluminum (Al)-doped ZnO (i-ZnO/AZO) window layer RF sputtering. The front contact Ni/Ag/Ni grid is evaporated through a shadow mask. Finally, the device is mechanically scribed with a stylus, to produce the individual test cells of 0.5 cm^2. The back contact is also reached by scribing. To avoid Mo oxidation, Silver (Ag) paste is put on the reached part of the Mo back contact immediately.

The finished ultra-thin CIGS SCs are characterized by current-voltage *(J-V)* measurement under standard test conditions of 1000 W/m^2 irradiation (AM 1.5 spectrum) at 25 °C. A one-diode equivalent circuit is used to interpret the
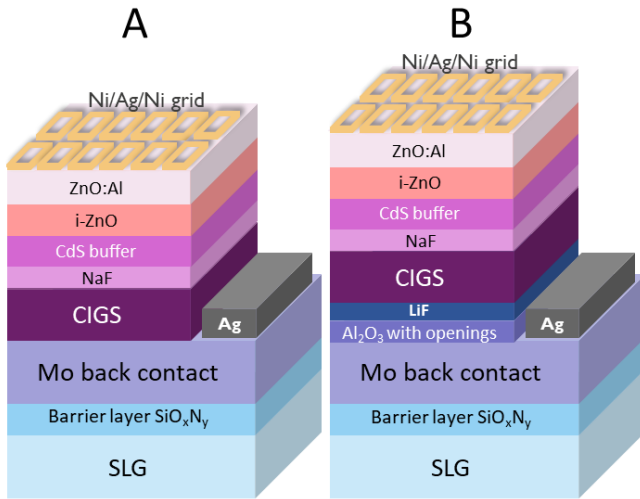
Figure 1. Schematic representation of the produced devices: A - reference sample, B - RSP sample.

obtained *J-V* characteristics. Using *J-V* curves, the V_{oc}, J_{sc}, *FF*, and efficiency values are deduced. For the External Quantum Efficiency (EQE) measurements, a SC is illuminated with monochromatic light of 350–1300 nm with 10 nm steps. More details on the data analysis are available in the Supplementary materials.

Atomic force microscopy (AFM) measurements were carried out using the NX10 AFM of Park systems. A SCM-PIT-V2 probe was used (Nominal k = 3 N/m) and the topography was measured using pinpoint mode. Pinpoint mode ensures a uniform gentle force applied to every pixel in the image, reducing lateral forces that act on the sample due to the lateral movement of the probe.

3. Results and discussion

3.1. Openings in the Al_2O_3 passivation layer

The described method of contact openings creation, i.e., selenization of alkali salt (LiF) on top of the Al_2O_3 passivation layer, succeeds to create openings in all tested alumina layer thicknesses from 6 to 30 nm, as confirmed by SEM images, see **Table 2**. The far view images demonstrate the

homogeneous distribution of the openings. The close view images show a typical openings profile, while the white bubble-like dots on the images are the not released openings. Experiments were conducted several times ensuring the repeatability of the method. To demonstrate that the open white structures observed with SEM are actually holes in the alumina layers reaching the molybdenum layer, AFM and I-V measurements were used. In **Figure 2**, an AFM topography image and depth profile are shown for a single opening in the thickest tested alumina layer of 30 nm. If the green line is followed simultaneous with the depth profile, it is seen that the opening follows a crater like profile going all the way down through the Mo layer to the back contact. The thickness of the hole is around 330-400 nm. As during the measurement, the needle goes all the way down to the SLG, so the scale includes the thickness of alumina (30nm) and Mo ($\approx$330nm) layers. Debris of about 150 nm thick can be seen around the hole, implying that the material within the hole is deposited around it. This latter is confirmed with the I-V curve for CIGS solar cell produced on the thickest tested alumina layer of 30 nm -which is given in Supplementary material on **Figure S4 -** to demonstrate the current collection through the openings.

As experimentally investigated, to obtain such openings in the alumina layer, three conditions should be satisfied simultaneously:

i) *enough LiF on top of the Al_2O_3 layer*

The volume of LiF solution (1.6M) used to spin-coat on 5×5 cm^2 sample must be at least 3.2 mL. If the amount of the salt is less, openings are not formed homogeneously, see Supplementary material **Figure S1-a**. While higher salt content nearly has no influence on the openings distribution, however, requires increased material wastage.
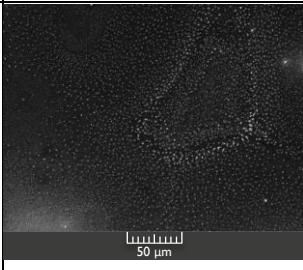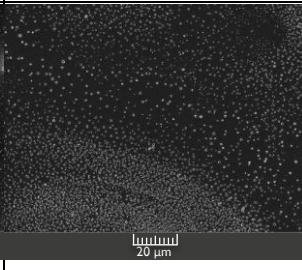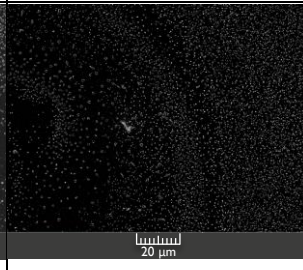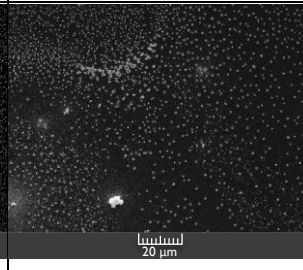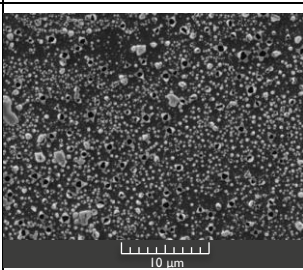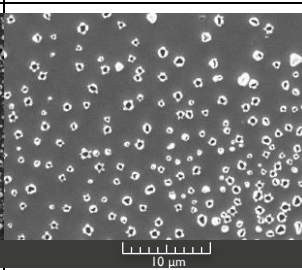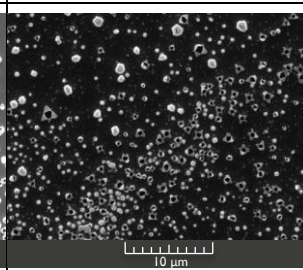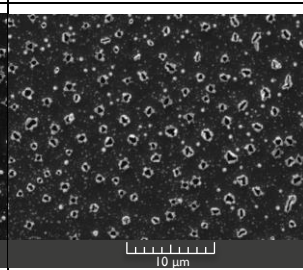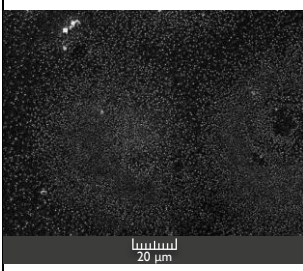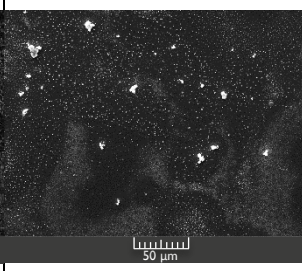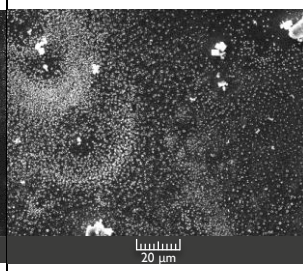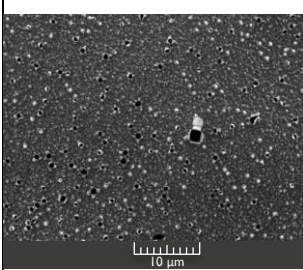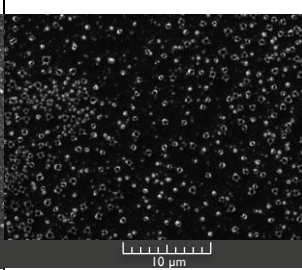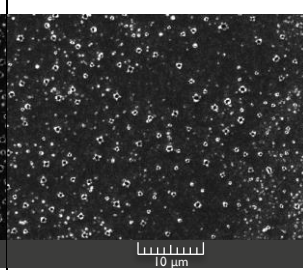
ii) *Selenium (Se) presence during annealing (selenization)*

Selenization can be done in pure Se or in H_2Se atmosphere. The second approach is preferable due to shorter process time, homogeneous openings distribution, and nearly zero defects on the surface, unlike the first approach, see Supplementary material **Figure S2**.
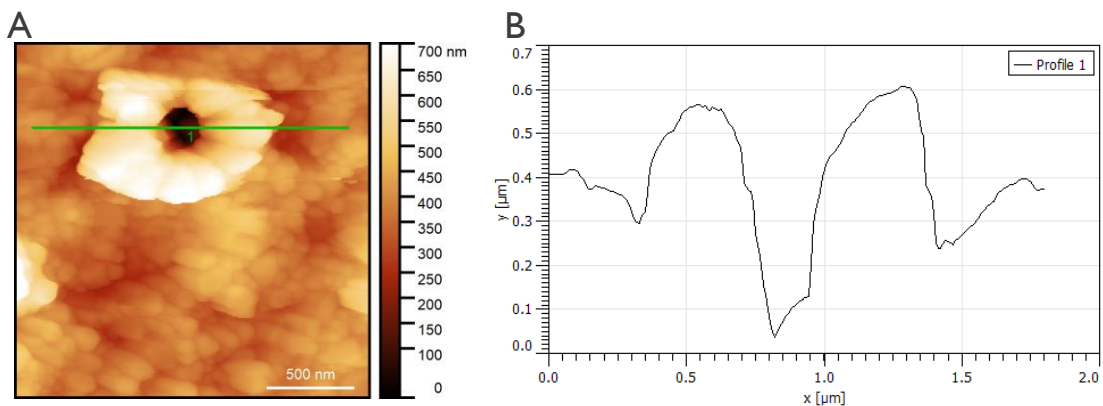
Figure 2. AFM image of the single opening in the 30 nm Al_2O_3 layer. A – topography image, B – depth profile measured along green line on A.

Table 2. SEM images of the openings released in the Al_2O_3 layer by LiF after selenization at time/temperature given in Table 1.

Al_2O_3 thickness	6 nm	8 nm	10 nm	15 nm
Far view image	50 µm	20 µm	20 µm	20 µm
Close view image	10 µm	10 µm	10 µm	10 µm

Al_2O_3 thickness	20 nm	25 nm	30 nm
Far view image	20 µm	50 µm	20 µm
Close view image	10 µm	10 µm	10 µm

iii) *enough annealing time and temperature*

Sufficient annealing time and temperature should be ensured, otherwise, openings formation is suppressed, see Supplementary material **Figure S1-b**. For the cost-efficient technique, it is important to keep the thermal budget as low as possible. Thus, the lowest temperature in combination with the shortest time that ensures the repeatable process of the openings creation with the homogeneous distribution is considered as an optimal. Moreover, the increase of the selenization temperature/time leads to the unwanted increase of the openings size. As a result, the optimal parameters, see **Table 1**, change slightly with the increasing thickness of the alumina layer.

The importance of homogeneous distribution of the openings and their size variation comes from the theoretical calculation based on analogy with Si SC with the Al_2O_3 passivation layer. Assuming the electron diffusion length of 0.75-1.5 µm, the openings' size of 200-400 nm with 1.5-3 µm pitch is considered as the optimal. For such distribution, the contacting area for CIGS SC should be around 2-5 % for the efficient current collection [12].

3.2. Mechanism of the openings' creation

It is probable that the origin of the openings creating is caused by degassing of alumina ALD layer. It is supposed that trapped gases inside the alumina layer elongate the alumina surface during the selenization process. Thus, the "bubbles" are created that can explode due to pressure difference and result in openings formation. Similar blistering of ALD Al_2O_3 layer as a result of gaseous desorption during temperature treatment was described previously, see [13]. However, such effect was observed only for a thick alumina layer and no blistering was observed for the thin one that is used in current research. The possible reason is that a thinner Al_2O_3 layer contains less trapped gases inside. Thus, additional gas encapsulation into thin alumina layer is needed, and possibly is provided by the high temperature local reactions between H_2Se and LiF. This hypothesis explains the requirement of LiF and H_2Se presence for the openings production.

Existing experience of local contact openings creating with alkali salts includes only fluorine salts. To check if the presence of Fluorine (F) during the selenization is essential for the openings production, experiments with NaCl instead of LiF are conducted. The 6 nm thick alumina layer is used for this experiment with the same selenization parameters as for LiF salt, i.e., 540 °C during 450 s in H_2Se atmosphere. The resulted SEM image after selenization is presented in Figure 3, where the openings are seen. The difference in the obtained openings profile comes from alkali element change, which is Na instead of Li, and non-optimized process for NaCl. As a result, it is found that alkali element of alkali salt has the key role in the openings formation process. However, the complete mechanism of openings production is still investigated.

3.3. Openings characterization

To investigate the openings' size and distribution, close view SEM images are further used for analysis with GWYDDION software [14], see Supplementary material.

If the distribution of the equivalent diameters of the openings plotted for each alumina layer thickness is investigated, it is seen that there is no correlation between the alumina layer thickness and the size of the created openings, see Supplementary material. Thus, in **Figure 4**, the summarized openings distribution is represented, while including the results from all tested samples regardless the Al_2O_3 layer thickness. According to **Figure 4**, at average
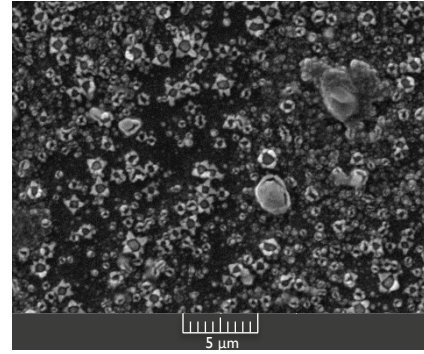
Figure 3. SEM images of the openings released in the 6 nm alumina layer with NaCl after selenization at 540 °C during 450 s in H_2Se atmosphere (10-kx magnification).

around 95% of the produced openings have the equivalent diameter of less 700 nm.

In **Table 3** the percentage of the released opened area in the different alumina layer thicknesses is given. Again, no dependence of the opened area values on the thickness of the passivation layer is observed. The average opened area of the alumina rear passivation layer is around 2.5%. The difference between the maximum and minimum values of the opened area is caused by a small size of the analyzed region (30 µm × 30 µm) presented on one SEM image, as high magnification images allow to precisely see and further characterize the single opening precisely. However, the general homogeneity of distribution is not represented on the close-view images. Consequently, it is essential to analyse at least four close-view images from one sample to estimate the representative average value of the opened area of the whole sample.

To summarize this part, the openings in the alumina layer produced by LiF selenization are nano-sized and well distributed over the sample. Moreover, the low average opened area value indicates that around 97.5% of the alumina layer is kept unopened. Based on theoretical predictions, such distribution is believed to be preferable for the rear surface passivation of the ultra-thin CIGS SC [15]. Moreover, this is the first time that nano-sized local contacts are created in a thick, i.e., 8-30 nm, ALD alumina layer using such a low-cost technique.

Table 3. The opened area (average, minimum, maximum values) released for the samples with the alumina passivation layer. The values for each Al_2O_3 layer thickness are indicated. The average values are calculated for 3 samples, while analyzing 4 images per sample. The minimum and maximum values are obtained from the single image analysis. The average value for all tested RSP samples is given.

Opened area, %	Al_2O_3 thickness, nm							Average for all RSP samples
	6	8	10	15	20	25	30	
Average	2.4%	2.7%	1.9%	1.8%	3.6%	2.2%	2.9%	2.5%
Minimum	0.5%	0.8%	0.9%	0.7%	1.4%	0.4%	0.9%	0.8%
Maximum	3.7%	5.4%	3.3%	3.0%	7.5%	3.5%	6.7%	4.7%
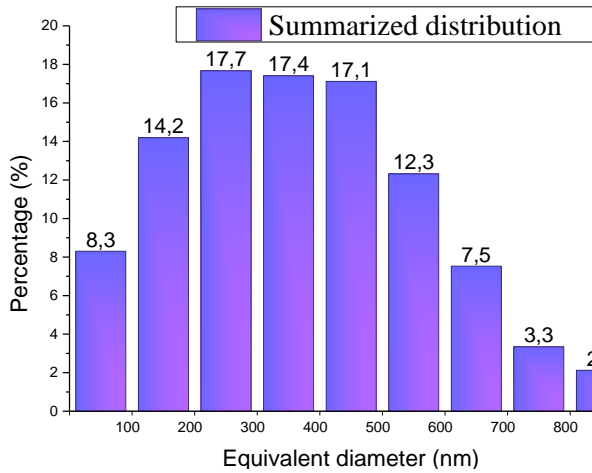
Figure 4. Total size distribution of the equivalent diameters of the openings created in the Al_2O_3 dielectric layer for all tested Al_2O_3 thicknesses from 6 nm to 30 nm.

3.4 Electrical and optical characterization of RSP CIGS SCs

To test the passivation effects of the Al_2O_3 dielectric layer with openings created by selenization of the LiF salt, one trial set of ultra-thin CIGS SCs is produced. The parameters of SCs are obtained from the *J-V* measurements, see **Figure 5**. For the most efficient cells, the J_{sc} values are extracted precisely from EQE spectral response, the procedure is described in

Supplementary material. These values are indicated as black dots in **Figure 5**-**A**.

The low V_{oc} values, see **Figure 5**-**B**, are observed for all RSP samples compared to the reference. However, it was expected that the introduced alumina passivation layer increases the V_{oc} due to reduced rear surface recombination and decreased concentration of the rear surface defects. The low V_{oc} values of the passivated samples might be caused by detrimental impact of LiF [16] on CIGS absorber layer composition and, thus, band gap. Moreover, double annealing of the dielectric layer can also affect the V_{oc} values due to degradation of alumina passivation properties, see more information in Supplementary material. These parts are still open to further investigation.

On the other hand, a slight increase of J_{sc} values of the RSP SCs compared to the reference is noticed in **Figure 5**-**A**. However, as explained in detail in [17], there is a barrier for photocurrent, and under AM 1.5 illumination, the high current density is not able to pass that barrier. However, the small current density can pass that barrier during the quantum efficiency measurement. Besides the difference in measured instrument, this minor increase can be related to either compositional and/or thickness differences, or the optical effect due to introduced rear passivation layer with nano-sized contact openings [18]. Since this is the first attempt of the solar cell production with this method, it is open for further improvements.

The increase in EQE response for long wavelengths implies the optical enhancement due to created passivation
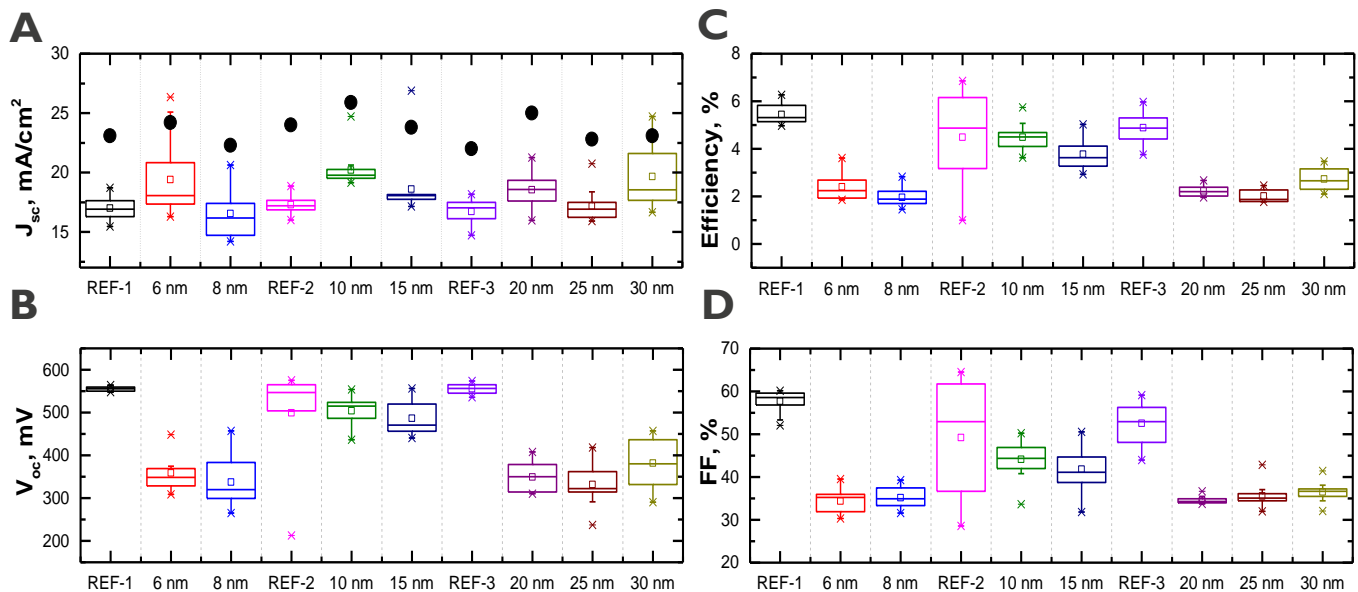
Figure 5. Statistical representation of the electrical parameters of the CIGS SCs obtained from the *J-V* measurements at global 1.5 AM spectrum. A) Short-circuit current J_{sc}, while the black circles represent J_{sc} values that are extracted from the EQE measurements for the most efficient cells. B) Open-circuit voltage V_{oc}. C) Efficiency of the cells. D) fill factor FF. The name of an RSP sample corresponds to the thickness of the introduced rear surface passivation layer, i.e., Al_2O_3 thickness. A reference (REF) sample is positioned before the RSP samples that are produced in the same run.

layer at rear surface [18], see Supplementary material **Figure S3**. For the samples with Al_2O_3 thickness of 6 nm, 10 nm, 20 nm, 25 nm, and 30 nm, the better EQE response for all wavelength above 550-600 nm is shown. For the thinner 6 nm and 10 nm alumina layers, this enhancement is mainly due to the light scattering from the edges of the nano-sized openings [15]. Starting from the 20 nm alumina layer, the increase of quantum efficiency is caused by both scattering from the edges of the nano-sized openings and rear surface reflectance improvement due to dielectric alumina layer [15]. However, the enhancement of the quantum response for the 8 nm and 15 nm RSP CIGS SCs is shown only for the longer wavelength, i.e., above 950 nm and 660 nm, respectively. Also, the recalculated J_{sc} values from EQE measurements for these samples are lower than for the reference samples, see **Figure 5**-**A**. However, it can be associated with the particular defects of the measured cells and is not connected with the passivation layer thickness.

Unfortunately, there is no FF and efficiency improvement of the passivated SCs compared to the reference samples, see **Figure 5**-**C** and -**D**. Since the creation of the openings is not yet a controllable process like lithography, the distribution, the size, and the population of the contact openings is not optimized. This fact, unfortunately, could lead to the decreased FF values for the passivated cells. This random process leaves regions with the insufficient opened area (see **Table 3**, minimum values) where openings are too small and separated at long distances. Thus, further optimization is needed to deduce the best value of the opened area of the passivation layer for the ultra-thin CIGS SC production. Moreover, as values of series and shunt resistance for reference and passivated samples are similar, see Supplementary material **Figure S5**, we suggest that low V_{oc} values of the RSP samples is responsible for FF and efficiency degradation. However, if the origin of the low V_{oc} values would be found and tackled, electrical improvement of the ultra-thin CIGS SCs is expected.

To conclude this part, the first trial set of the ultra-thin RSP CIGS SCs with the Al_2O_3 rear surface passivation layer of thicknesses from 6 to 30 nm were produced, and decent current collection was provided through contact openings. However, we could not detect the passivation effect for all set of RSP samples. Moreover, we could not find any dependence of the electrical and optical parameters of the ultra-thin CIGS SCs on the Al_2O_3 layer thickness. For the further investigation, the origin of the low V_{oc} values needs to be found, and the SC production process should be optimized.

4. Conclusions and outlook

This work presents the method of local nano-sized contact openings creation in the Al_2O_3 rear surface passivation layer by using LiF salt selenization. The described method is a unique, cost-effective way of contacting through the passivation layer that succeeds to create contact openings in the ALD alumina layer of the thickness up to 30 nm. However, the upper limit of the Al_2O_3 layer thickness is not yet established and is open for the further study. As confirmed by SEM images, the resulted openings are nano-sized, i.e., at average more than 95% of the openings is less 700 nm in diameter, and homogeneously distributed over the sample. At the same time most of the Al_2O_3 surface is kept unopened to ensure the effective passivation, while at average 2.5% of surface area is left for contacting.

A one trial set of ultra-thin CIGS SC is produced on the passivated substrates with the Al_2O_3 layer thicknesses of 6 nm, 8 nm, 10 nm, 15 nm, 20 nm, 25 nm, and 30 nm. The gained results demonstrate adequate current collection for all alumina layer thicknesses up to 30 nm and thus the effectiveness of the applied method for the openings creation. Moreover, for longer wavelengths, EQE response is enhanced by (i) enhanced rear surface reflectance, and (ii) light scattering from the openings' edges. However, due to the low V_{oc} values, the FF and efficiency of the RSP cells are degraded. Thus, the source of the V_{oc} values decrease in the passivated samples needs to be investigated as well as the way of the ultra-thin CIGS SCs production on top the described passivation layer needs to be repeated and optimized.

Nevertheless, the described method of LiF selenization on top of Al_2O_3 layer has a potential for further use in ultra-thin CIGS SCs. The main reasons for industrial viability are the followings: repeatability of the process, potentially quick and low-cost processing, possibility to create contact openings in the relatively thick alumina layer up to 30 nm. As the increased thickness of the passivation layer provides the better passivation effect [15], [19], further reducing of the CIGS absorber layer thickness while keeping its performance is possible.

Acknowledgements

References

[1]   M. A. Green, E. D. Dunlop, J. Hohl-Ebinger, M. Yoshita, N. Kopidakis, and A. W. Y. Ho-Baillie, "Solar cell efficiency tables (Version 55)," *Prog. Photovoltaics Res. Appl.*, vol. 28, no. 1, pp. 3–15, Jan. 2020, doi: 10.1002/pip.3228.

[2]   J. Ramanujam and U. P. Singh, "Copper indium gallium selenide based solar cells - A review," *Energy and Environmental Science*, vol. 10, no. 6. Royal Society of Chemistry, pp. 1306–1319, Jun. 01, 2017, doi: 10.1039/c7ee00826k.

[3]   N. Naghavi *et al.*, "Ultrathin Cu(In,Ga)Se2 based solar cells," *Thin Solid Films*, vol. 633, pp. 55–60, Jul. 2017, doi: 10.1016/j.tsf.2016.11.029.

[4]   R. Kotipalli, B. Vermang, J. Joel, R. Rajkumar, M. Edoff,

and D. Flandre, "Investigating the electronic properties of Al2O3/Cu(In,Ga)Se2 interface," *AIP Adv.*, vol. 5, no. 10, p. 107101, Oct. 2015, doi: 10.1063/1.4932512.

[5]   B. Vermang *et al.*, "Introduction of Si PERC rear contacting design to boost efficiency of Cu(In,Ga)Se2solar cells," *IEEE J. Photovoltaics*, vol. 4, no. 6, pp. 1644–1649, 2014, doi: 10.1109/JPHOTOV.2014.2350696.

[6]   B. Vermang *et al.*, "Employing Si solar cell technology to increase efficiency of ultra-thin Cu(In,Ga)Se $_2$ solar cells," *Prog. Photovoltaics Res. Appl.*, vol. 22, no. 10, pp. 1023–1029, Oct. 2014, doi: 10.1002/pip.2527.

[7]   P. M. P. Salomé *et al.*, "Passivation of Interfaces in Thin Film Solar Cells: Understanding the Effects of a Nanostructured Rear Point Contact Layer," *Adv. Mater. Interfaces*, vol. 5, no. 2, p. 1701101, Jan. 2018, doi: 10.1002/admi.201701101.

[8]   G. Birant, J. de Wild, M. Meuris, J. Poortmans, and B. Vermang, "Dielectric-Based Rear Surface Passivation Approaches for Cu(In,Ga)Se2 Solar Cells—A Review," *Appl. Sci.*, vol. 9, no. 4, p. 677, Feb. 2019, doi: 10.3390/app9040677.

[9]   D. Ledinek, O. Donzel-Gargand, M. Sköld, J. Keller, and M. Edoff, "Effect of different Na supply methods on thin Cu(In,Ga)Se2 solar cells with Al2O3 rear passivation layers," *Sol. Energy Mater. Sol. Cells*, vol. 187, pp. 160–169, Dec. 2018, doi: 10.1016/j.solmat.2018.07.017.

[10] G. Birant *et al.*, "Innovative and industrially viable approach to fabricate AlOx rear passivated ultra-thin Cu(In, Ga)Se2 (CIGS) solar cells," *Sol. Energy*, vol. 207, pp. 1002–1008, Sep. 2020, doi: 10.1016/j.solener.2020.07.038.

[11] M. Nakamura, K. Yamaguchi, Y. Kimoto, Y. Yasaki, T. Kato, and H. Sugimoto, "Cd-Free Cu(In,Ga)(Se,S)2 thin-film solar cell with record efficiency of 23.35%," *IEEE J. Photovoltaics*, vol. 9, no. 6, pp. 1863–1867, Nov. 2019, doi: 10.1109/JPHOTOV.2019.2937218.

[12] B. Vermang, V. Fjällström, J. Pettersson, P. Salomé, and M. Edoff, "Development of rear surface passivated Cu(In,Ga)Se2 thin film solar cells with nano-sized local rear point contacts," *Sol. Energy Mater. Sol. Cells*, vol. 117, pp. 505–511, Oct. 2013, doi: 10.1016/j.solmat.2013.07.025.

[13] O. Beldarrain, M. Duch, M. Zabala, J. M. Rafí, M. B. González, and F. Campabadal, " Blistering of atomic layer deposition Al 2 O 3 layers grown on silicon and its effect on metal–insulator–semiconductor structures ," *J. Vac. Sci. Technol. A Vacuum, Surfaces, Film.*, vol. 31, no. 1, p. 01A128, Jan. 2013, doi: 10.1116/1.4768170.

[14] "Gwyddion – Free SPM (AFM, SNOM/NSOM, STM, MFM, …) data analysis software." http://gwyddion.net/ (accessed Aug. 06, 2020).

[15] B. Vermang, V. Fjallström, X. Gao, and M. Edoff, "Improved rear surface passivation of Cu(In,Ga)Se2 solar cells: A combination of an Al2O3 rear surface passivation layer and nanosized local rear point contacts," *IEEE J. Photovoltaics*, vol. 4, no. 1, pp. 486–492, Jan. 2014, doi: 10.1109/JPHOTOV.2013.2287769.

[16] S. Ishizuka and P. J. Fons, "Lithium-Doping Effects in Cu(In,Ga)Se2 Thin-Film and Photovoltaic Properties," *ACS Appl. Mater. Interfaces*, vol. 12, no. 22, pp. 25058–25065, Jun. 2020, doi: 10.1021/acsami.0c06284.

[17] R. Scheer and H.-W. Schock, "Appendix A: Frequently Observed Anomalies," in *Chalcogenide Photovoltaics*, Weinheim, Germany: Wiley-VCH Verlag GmbH & Co. KGaA, 2011, pp. 305–314.

[18] S. S. Hegedus and W. N. Shafarman, "Thin-film solar cells: Device measurements and analysis," *Prog. Photovoltaics Res. Appl.*, vol. 12, no. 2–3, pp. 155–176, Mar. 2004, doi: 10.1002/pip.518.

[19] W. W. Hsu *et al.*, "Surface passivation of Cu(In,Ga)Se 2 using atomic layer deposited Al 2O 3," *Appl. Phys. Lett.*, vol. 100, no. 2, p. 023508, Jan. 2012, doi: 10.1063/1.3675849.